COMMUNICATION

Concordance of Residual Dipolar Couplings, Backbone Order Parameters and Crystallographic *B*-factors for a Small α/β Protein: A Unified Picture of High Probability, Fast Atomic Motions in Proteins

G. Marius Clore[1]* and Charles D. Schwieters[2]*

[1]*Laboratory of Chemical Physics Building 5, National Institute of Diabetes and Digestive and Kidney Diseases, National Institutes of Health, Bethesda MD 20892-0520, USA*

[2]*Division of Computational Bioscience, Building 12A Center for Information Technology, National Institutes of Health, Bethesda, MD 20892-5624, USA*

*Corresponding author

Using ensemble refinement of the third immunoglobulin binding domain (GB3) of streptococcal protein G (a small α/β protein of 56 residues), we demonstrate that backbone (N–H, N–C', Cα–Hα, Cα–C') residual dipolar coupling data in five independent alignment media, generalized order parameters from ^{15}N relaxation data, and *B*-factors from a high-resolution (1.1 Å), room temperature crystal structure are entirely consistent with one another within experimental error. The optimal ensemble size representation is between four and eight, as assessed by complete cross-validation of the residual dipolar couplings. Thus, in the case of GB3, all three observables reflect the same low-amplitude anisotropic motions arising from fluctuations in backbone ϕ/ψ torsion angles in the picosecond to nanosecond regime in both solution and crystalline environments, yielding a unified picture of fast, high-probability atomic motions in proteins. An understanding of these motions is crucial for understanding the impact of protein dynamics on protein function, since they provide part of the driving force for triggered conformational changes that occur, for example, upon ligand binding, signal transduction and enzyme catalysis.

Published by Elsevier Ltd.

Keywords: protein dynamics; residual dipolar couplings; multiple alignment media; relaxation order parameters; crystallographic *B*-factors

Protein dynamics is central to protein function and is a prerequisite for catalysis, recognition and binding to both small molecule ligands and macromolecules, and protein signaling.[1–8] Briefly, it is understood that protein motions can be divided into three main categories:[6] (i) small random atomic fluctuations on the sub-picosecond timescale (e.g. bond librations) that are, in general, uniform throughout the protein; (ii) correlated motions involving the concerted movement of small or large groups of atoms that can span the picosecond to second timescale (e.g. crank-shaft motions along the polypeptide backbone, which are both frequent and fast; aromatic ring flips, which are fast but infrequent; local unfolding, which is slow and infrequent; and interdomain motions); and (iii) triggered conformational changes. The first category always represents random, essentially axially symmetric, excursions about an equilibrium conformation and is driven by the inherent kinetic energy of a protein. The second category is also driven by inherent kinetic energy and can involve either random excursions about an equilibrium conformation or transitions from one equilibrium state (or sub-state) to another. The third category always involves a transition from one equilibrium state to another and, while triggered by an external event such as ligand binding, still requires inherent kinetic energy and, hence, the existence of the other two motional classes, to take place.

In the crystalline state, crystallographic temperature (*B*) factors provide a measure of motional amplitudes arising from the combined effects of dynamic and static disorder within the crystal lattice.[6,9] Normally, the resolution of protein

crystallography is not sufficient to yield anything other than isotropic *B*-factors, which simply represent a Gaussian distribution about the equilibrium position in which a given atom can be located. For ultra-high resolution (<1 Å) crystal structures, however, anisotropic *B*-factors can be obtained, which provide a picture of the direction of the atomic motions. In solution, heteronuclear relaxation measurements can, in principle, yield motional information for almost all heavy-atoms.[1–5] Amplitudes of motions, expressed as model-free order parameters,[10] can be probed on timescales ranging from picoseconds to nanoseconds by means of laboratory-frame experiments,[5] while the dynamics of slower motions ranging from microseconds to milliseconds can be analyzed from rotating frame measurements.[11] However, model-free interpretation of relaxation measurements does not yield a physical picture of the nature of the motions.

More recently, residual dipolar couplings (RDCs) have been suggested as an additional approach for analyzing motional amplitudes over the entire picosecond to millisecond timescale.[12–23] RDCs are measured by inducing a very small degree of alignment ($\sim 10^{-3}$) of the protein in the magnetic field, typically by dissolving the protein in a dilute liquid crystalline medium.[24] RDCs provide a direct measure of the orientation of atomic vectors to an external alignment tensor and provide a very powerful tool in NMR structure determination. The simplest and most straightforward application of RDCs to dynamics involves the detection of large-scale inter-domain motions, whose presence is easy to ascertain, since the alignment tensor for the two domains will be different.[25–27] By measuring RDCs in several alignment media possessing different alignment tensors (i.e. different orientations and/or rhombicity), it is possible, in principle, to derive detailed information on the dynamics of individual vectors since, in the presence of anisotropic motions, the RDCs in the different media will not be consistent with a single structure.

Early studies based on various mathematical model-free formalisms of motion suggested that RDCs provided evidence for much larger-scale backbone motions than those reflected in the order parameters derived from ^{15}N relaxation measurements, leading the authors to conclude that proteins exhibit large-scale concerted motions that are present all the time over the nanosecond to millisecond range; that is, these postulated motions are frequent and of high probability.[12–21,28] If this were true, it would represent a paradigm shift in our understanding of protein motions. More recently, we proposed a simple, intuitive approach for analyzing RDCs.[22,23] Rather than assume that the RDCs can be represented by a single structure, we sought to represent the RDC data by an ensemble of structures in which the overall calculated RDCs for the ensemble are given by the average of the calculated RDCs of the individual

members of the ensemble. No assumption is made with regard to either structure or the alignment tensor, since the coordinates are refined, and the magnitude and orientation of the alignment tensor are optimized simultaneously.[22] We do, however, assume a single alignment tensor, an assumption that is valid providing either the motions are faster than the rotational correlation time of the molecule or, if the motions are slower than this limit, they do not affect the overall shape of the molecule. (Note that the assumption of a single alignment tensor also applied to the earlier studies.[12–21,28]) Using this approach, we were able to show that the order parameters, S^2_{NH} (dipolar), derived from RDCs measured in multiple alignment media, are correlated (with a correlation coefficient of ~ 0.8) with those from relaxation measurements, S^2_{NH} (relaxation), and the latter are approximately 0.9 times smaller than the former.[23] Since S^2_{NH} (relaxation) is a product of axial and anisotropic components arising from bond librations and conformational motions (about the backbone torsion angles), respectively, and since our analysis of the RDCs is essentially insensitive to bond librations (which can be considered to be constant throughout the polypeptide chain), it follows that S^2_{NH} (libration) ~ 0.9, in agreement with molecular dynamics simulations.[29] The calculation of S^2_{NH} (relaxation) from experimental relaxation data generally makes use of an equilibrium N–H bond distance ($R_{\mathrm{NH,eq}}$) of 1.02 Å derived from neutron diffraction.[5] Our findings[23] therefore imply that the effective, vibrationally corrected, N–H bond length ($r_{\mathrm{NH,eff}}$), given by $(R_{\mathrm{NH,eq}}/S^2)^{1/6}$,[30] is 1.04 Å, a value that coincides exactly with the vibrationally corrected N–H bond length derived from N–H and N–C' RDC measurements in two alignment media.[31] In addition, this analysis of the RDC data is able to provide a physical picture of the motions and to demonstrate directly the presence of correlated short-range (crank-shaft motions with anti-correlation of ϕ_i and ψ_{i-1}) and long-range (between residues close in space but far apart in the sequence) motions.[23]

Very recently, ensemble averaged (using an ensemble size of 16) molecular dynamics has been suggested as a means of simultaneously refining protein structure and dynamics from nuclear Overhauser effect (NOE) and relaxation order parameter restraints in the context of the CHARMM empirical force field including the implicit treatment of solvent.[32,33] Since the generalized order parameters are a direct measure of angular amplitudes of motion for specific bond vectors, this approach should, in principle, yield an estimate of the expected distribution of structures consistent with atomic motions on the picosecond to nanosecond timescale. It should be noted, however, that interproton distance restraints derived from NOE data are $\langle r^{-6} \rangle^{-1/6}$ averages, and consequently NOE refinement does not cross-validate with ensemble sizes larger than 2.[34,35] Hence, the only effective restriction on atomic positions arises from the order parameter restraints and the full empirical force

field, which is akin to carrying out a molecular dynamics simulation in which atomic displacements are restricted to lie within a tube of variable diameter.

The question we pose here is whether RDC measurements in multiple alignment media, relaxation measurements and crystallographic *B*-factors reflect different sorts of motion (in terms of magnitude and timescale), as has been proposed,[12–21,28] or whether these three independent physical measurements can be explained by a unified picture of concerted motions occurring on the sub-nanosecond to nanosecond timescales. To this end, we have carried out a simultaneous ensemble refinement of RDCs, NH order parameters and crystallographic *B*-factors using complete RDC cross-validation for the small α/β protein GB3 (the third IgG-binding domain of streptococcal protein G).

GB3 is 56 residues in length, and comprises a mixed parallel/antiparallel four stranded β-sheet with a $-1, +3x, -1$ topology, on top of which lies a single α-helix.[36] The RDC data, which are of very great accuracy, represent four backbone vectors (N–H, N–C′, Cα–Hα, and Cα–C′) per residue measured in five different alignment media (bicelles, polyethylene glycol/hexanol, phage pf1, positively charged gel and negatively charged gel);[37] the crystallographic *B*-factors are obtained from a highly refined, room temperature 1.1 Å resolution crystal structure,[38] and can therefore be deemed to be rather accurate; and finally, the S^2_{NH} (relaxation) order parameters are derived from very careful ^{15}N relaxation measurements and N–H atomic coordinates calculated from the high-resolution crystal structure, and therefore accurately take into account axially symmetric diffusion anisotropy arising from the ellipsoidal shape of the protein.[39] Because GB3 is a relatively rigid protein, as judged from relaxation measurements, it provides an ideal platform for an in-depth analysis of small-scale concerted motions, which are at the core of all protein motions. Thus, even GB3 can undergo conformational transitions, as is evident by small but significant backbone displacements in one of the β-strands upon binding its target, the Fc region of immunoglobulins.[38]

The potentials used for ensemble refinement against RDCs have been described.[22,23] In the current work, two additional potential terms for the S^2 order parameter and the crystallographic *B*-factor were introduced into Xplor-NIH.[40]

The order parameter S^2 associated with motion of a rigid bond vector in an ensemble of size N_e is calculated as:[30]

$$S^2 = \frac{1}{2} \sum_{i=1}^{N_e} \sum_{j=1}^{N_e} w_i w_j [3(\mathbf{u}_i \cdot \mathbf{u}_j)^2 - 1] \quad (1)$$

where $\mathbf{u}_i$ is a unit vector along the bond in question in ensemble member i, and w_i is the weight associated with ensemble member i (normally

$1/N_e$). The associated energy term, E_{order}, used in ensemble refinement is given by:

$$E_{order} = w_{order}(S^2 - S^2_{obs})^2 \quad (2)$$

where S^2_{obs} is the observed order parameter for a given bond vector and w_{order} is a scale factor.

The crystallographic *B*-factor for atom k is given by:[9]

$$B = 8\pi^2 \sum_{i=1}^{N_e} w_i |q_{ik} - \bar{q}_k - Q_i + \bar{Q}|^2 \quad (3)$$

where q_{ik} is the position of atom k in ensemble member i, and $\bar{q}_k$ is this atom's ensemble averaged position. Q_i is the center of mass of the molecular structure in ensemble i, and $\bar{Q}$ is the ensemble-averaged center of mass. These latter two terms are included so that the calculated *B*-factor is invariant to intra-ensemble translations. The associated energy term, E_{Bfact}, is given by:

$$E_{Bfact} = w_{Bfact}(B - B_{obs})^2 \quad (4)$$

where B_{obs} is the observed *B*-factor value and w_{Bfact} is a scale factor. The *B*-factor restraint term supercedes the arbitrary and uniform relative atomic position term used previously,[22,23] and ensures consistency of the atomic r.m.s. displacement amplitudes as measured by crystallography with the angular motional amplitudes reflected by the RDCs and relaxation order parameters.

The simulated annealing protocol, comprising both torsion angle and cartesian coordinate dynamics as well as cartesian coordinate minimization, followed closely that described previously (including the values of the scale factors for the various terms in the target function).[23] In addition, the scale factor w_{Bfact} was set to 0.1 kcal mol^{-1} Å^{-4} for backbone (N, Cα, C′, O) atoms and 0.02 kcal mol^{-1} Å^{-4} for side-chain atoms. while the scale factor for S^2_{NH} was increased geometrically from 0.01 to 0.3. The published S^2_{NH} values, derived from the ^{15}N relaxation data and crystallographic coordinates with an axially symmetric diffusion tensor, were obtained using a bond length of 1.02 Å,[34] and were therefore corrected for an effective equilibrium bond length of 1.04 Å, by multiplying their values by a factor of $(r_{eff,NH}/R_{eq,NH})^6 = 1.124$.[30] The target function, with the exception of the two new terms and the omission of the relative atomic position term[22] (which is no longer necessary owing to the presence of the *B*-factor restraints), was identical with that used previously and comprises terms for the experimental restraints (RDCs, loose backbone and side-chain torsion angle restraints, backbone hydrogen bonding distance restraints, S^2_{NH} order parameter restraints and *B*-factor restraints for all heavy-atoms), covalent geometry (bond lengths, bond angles and improper torsions, weighted as described[23] to allow for small variations in the geometry of the peptide bond[37]) and non-bonded contacts (quartic van der Waals repulsion term,

radius of gyration restraint,[41] multi-dimensional torsion angle database potential of mean force,[42] an empirical backbone hydrogen bonding potential derived from protein crystal structures,[43] and an overall shape term[22]). One other minor modification was incorporated with regard to the RDC refinement, in that the optimized D_a and rhombicity values for the five alignment tensors were constrained to be absolutely identical for all members of a given ensemble, rather than restrained by harmonic spread terms.[22] Calculations were carried out with ensemble sizes of $N_e = 1, 2, 4, 8$ and 16, and 20 sets of calculations were carried out for each ensemble. The RDCs were subject to complete cross-validation as follows. The N–H RDCs from one medium, the N–C$'$ from a second medium, the C$^\alpha$–H$^\alpha$ for a third medium and the C$^\alpha$–C$'$ from a fourth medium were left out and used as the free RDC data set. These were permuted to generate eight different combinations of free RDC datasets. (Note that complete permutation would generate 2880 possible combinations and this is far too large a number for computational purposes; eight combinations, which represent a reasonable number for computational tractability, were therefore randomly chosen for the calculations. This number was deemed sufficiently extensive for the purposes of cross-validation, particularly as essentially the same results were obtained for each combination). Thus, for each ensemble size, a total of 160 N_e structures were calculated and the results reported represent the averages and standard deviations for these structures. All the calculated structures display very small deviations from idealized covalent

geometry, exhibit >94% of residues in the most favorable region of the Ramachandran map with all remaining residues in additionally allowed regions, and favorable non-bonded contacts (with <4 bad contacts per 100 residues).[44]

The data in Figure 1 show a plot of the r.m.s. difference between observed and calculated values of the free and working RDC data sets, the S^2_{NH} (relaxation) order parameters, the backbone B-factors, and the free (i.e. not included as restraints) $^3J_{HN\alpha}$ coupling constants as a function of ensemble size. The RDCs and $^3J_{HN\alpha}$ coupling constants are structural parameters that can usually be described using a single structure representation. These observables, however, may be modulated by motion, although, in general, both are relatively insensitive to small-scale motions. The S^2_{NH} (relaxation) order parameters and B-factors are direct metrics of angular and atomic displacement motions, respectively, and can therefore be described only by an ensemble representation (i.e. $N_e \geq 2$). For both the working and free RDC data sets, there is large improvement in agreement between observed and calculated values as N_e is increased from 1 (single structure representation) to 2 (ensemble structure representation), providing a clearcut demonstration that these parameters are modulated by motion; there is some further improvement as N_e is increased from 2 to 4, and thereafter minimal, incremental improvements as N_e is increased from 4 to 16. These findings are in agreement with our previously published results.[22,23] The free $^3J_{HN\alpha}$ coupling constants also show improvement from $N_e = 1$ to 2, and thereafter
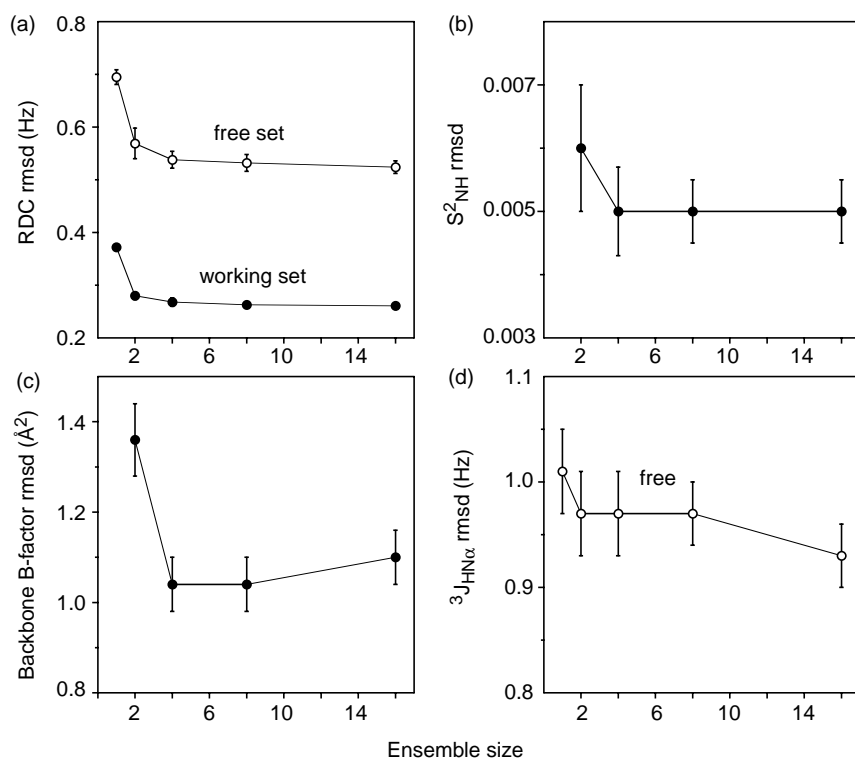
Figure 1. Dependence of the r.m.s. difference between observed and calculated values for various NMR observables as a function of ensemble size (N_e): (a) working and free RDC data sets; (b) the S^2_{NH} (relaxation) order parameter restraints; (c) the backbone B-factor restraints (N, C$^\alpha$, C$'$ and O atoms); and (d) the free $^3J_{HN\alpha}$ coupling constant dataset. Note that free datasets are not included in the refinement and are represented by open circles. Restraints included in the refinement (working datasets) are denoted by filled circles.

only small incremental improvements as N_e is increased further. In the case of S^2_{NH} (relaxation) order parameters and backbone *B*-factors, there is a significant improvement in agreement between observed and calculated values as N_e is increased from 2 to 4, and thereafter no significant change is observed as N_e is increased further. One can therefore conclude that the optimal size of N_e required to represent all the data is between 4 and 8, and the small improvements in agreement for the working RDC data sets up to $N_e=16$ are not due to over-fitting of the data. The backbone atomic r.m.s. difference from the mean coordinates for each ensemble calculation is ~ 0.3 Å and remains essentially unchanged for $N_{e=}2$ to 16. The latter is a direct reflection of the impact of the *B*-factor restraints. The backbone atomic r.m.s. difference between the mean coordinates for the $N_e=2$ to 16 ensembles to the mean coordinates for the $N_e=1$ calculations is ~ 0.2 Å, and between the mean coordinates for the $N_e=1$ to 16 ensembles to the X-ray coordinates ranges from 0.5–0.6 Å.

Figure 2 displays correlation plots of observed *versus* calculated values ($N_e=8$) for the working and free RDCs, the S^2_{NH} (relaxation) order parameters and the backbone *B*-factors. As is evident from the plots, the correlations for both the working and free RDCs and the order parameters are very high (correlation coefficients of 0.997–0.998) with a slope of 1.0. For only a single residue, Gly41, which exhibits the smallest measured S^2_{NH} (relaxation) order parameter (Figure 2(c)) and is located in the loop (residues 37–41) connecting the single α-helix

to the third β-strand, the calculated value of S^2_{NH} is slightly lower than the observed one (0.53 *versus* 0.56 ± 0.01). This might possibly be interpreted to suggest some additional contribution from low-amplitude motion on a timescale longer than the rotational correlation time (~ 4 ns) for Gly41. However, the value of S^2_{NH} (relaxation) for Gly41 is quite dependent on the diffusion model (axially symmetric *versus* fully anisotropic) used to fit the experimental relaxation data, and its S^2_{NH} (relaxation) value is reduced to 0.52 ± 0.01 for the fully anisotropic diffusion model.[39] The scatter is a little larger for the backbone *B*-factors with a correlation coefficient of 0.94 but is within the uncertainties of the experimentally determined *B* values.

Observable RDCs are a consequence of the small degree of alignment of the protein in the magnetic field arising from extremely weak, highly transient interactions between the protein and the various alignment media.[24] There always exists the possibility, however remote, that these very weak interactions could potentially induce structural distortions of the same magnitude as the motional amplitudes derived from the ensemble calculations. This possibility, however, is excluded by the near-perfect agreement between calculated and experimental order parameters (Figure 2(c)) and calculated and experimental RDCs (Figure 2(a) and (b)), since the relaxation order parameters are measured in the absence of any alignment media.

Another set of calculations for $N_e=4$ and 8 was also carried out using the S^2_{NH} (relaxation) order parameters uncorrected for bond length (i.e. the
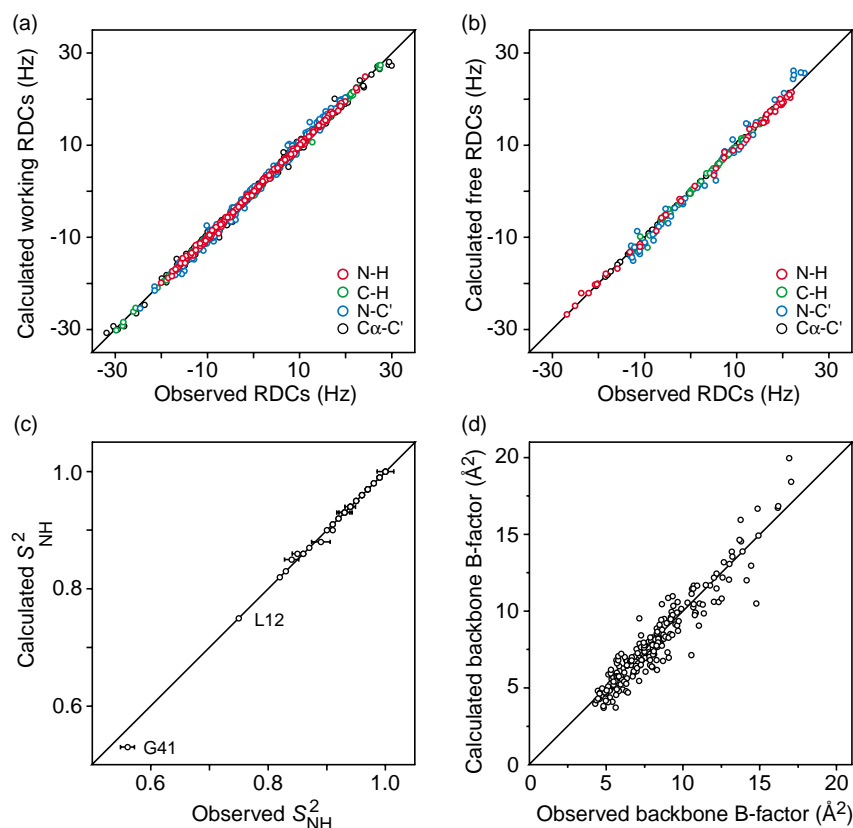
Figure 2. Comparison of observed and calculated values of NMR observables for an ensemble size of $N_e=8$. (a) Working normalized RDCs, (b) free normalized RDCs, (c) S^2_{NH} (relaxation) order parameters and (d) backbone *B*-factors. In (a) and (b) the $C^α$–$H^α$ (green), N–C' (blue) and $C^α$–C' (black) RDCs have been normalized to the same scale as the N–H (red) RDCs according to bond length and gyromagnetic ratios. The results shown are derived from a set of 20 independent $N_e=8$ calculations in which the free RDC data set (i.e. not included in refinement) comprised RDCs omitted from the various alignment media as follows: the N–H RDCs from bicelles, the $C^α$–$H^α$ RDCs from the negatively charged gel, the $C^α$–C' RDCs from the positively charged gel and the N–C' RDCs from phage pf1. The horizontal bars in (c) indicate the standard deviations for the experimentally determined S^2_{NH} (relaxation) order parameters.

reported values calculated with $r_{NH}=1.02$ Å) for a single (arbitrarily chosen) RDC cross-validation set (in which the N–H RDCs for bicelles, the N–C′ RDCs in pf1, the C^α–H^α RDC in negative gel and the C^α–C′ RDC in positive gel were omitted). The r.m.s. difference between observed and calculated working RDCs was the same for the calculations with the corrected and uncorrected S_{NH}^2 (relaxation) order parameter restraints. However, the agreement between observed and calculated free RDCs and between observed and calculated S_{NH}^2 (relaxation) values was 20% and 60% worse, respectively, in the calculations using the uncorrected S_{NH}^2 (relaxation) restraints. In addition, the deviations from idealized geometry for bond angles and improper torsions were 4–7% and 11–16%, respectively, higher for the structures calculated with the uncorrected than the corrected S_{NH}^2 (relaxation) restraints. These larger deviations from idealized covalent geometry probably represent a partial attempt to account for the bond libration component in the uncorrected S_{NH}^2 (relaxation) restraints but cannot fully do so with the force constants employed here for the geometrical terms.

In conclusion, the present data demonstrate that, for a small, relatively rigid, protein such as GB3, the RDCs in multiple alignment media, the model free S_{NH}^2 (relaxation) generalized order parameters from ^{15}N relaxation measurements, and the backbone *B*-factors from a high-resolution, room temperature crystal structure are entirely consistent with one another, and reflect the same low-amplitude, high-probability, anisotropic motions arising from fluctuations in backbone ϕ/ψ torsion angles on a timescale in the picosecond to nanosecond regime in both solution and crystalline environments that can be well represented by ensemble sizes of $N_e=$ 4–8. Although all three observables reflect the same motions, highly accurate RDCs in multiple alignment media can provide significant new insights into the nature of these motions, since ensemble refinement, of the type described here, permits one to obtain a direct physical picture for the motions of different bond vectors and to ascertain the presence of correlated atomic motions.[23]

The results presented here also have considerable impact with regard to the widespread use of RDCs as long-range orientational restraints in NMR macromolecular structure determination.[24] Specifically, one can conclude that, for most practical purposes, it is perfectly legitimate to use RDCs for structure refinement in the context of a single structure representation, since, for the majority of NMR structure determinations, the average atomic r.m.s. difference from the mean coordinate positions (i.e. the precision) is generally larger than the amplitude of the motions detected by the RDCs, relaxation measurements and crystallographic *B*-factors. Moreover, the accuracy of the measured RDCs required to analyze motions is much higher than that required for NMR structure determination.

In contrast to bond librations, which are uniform along the polypeptide chain and axially symmetric, high-probability conformational fluctuations in the sub-nanosecond regime are non-uniform, anisotropic and exhibit distinct variations along the polypeptide chain. In the case of GB3, the variations are relatively small, as expected given the very high degree ($\sim$90%) of secondary structure content. GB3 contains two regions that exhibit relatively large amplitude motions ($S^2<0.8$) on the sub-nanosecond timescale, one in the turn connecting strands β1 and β2, and the other in the loop connecting the C-terminal end of the single α-helix to strand β3. Perhaps more interesting are two other regions that exhibit lower than average order parameters: the N-terminal half of strand β2 and the N-terminal region of the α-helix. This increased mobility is suggestive, since these two regions comprise the site of interaction of GB3 with its biological target, the Fc region of immunoglobulins, and it is precisely the backbone of these two regions that exhibit clearcut, albeit small, structural differences between the free and bound states of GB3.[38] Thus, it may be that the presence of larger than average atomic fluctuations at the sub-nanosecond level are an important component for effecting triggered conformational changes that are a key component of the function of most proteins.

Here, we have focused on motions that occur on a timescale shorter than the rotational correlation time. However, RDCs are potentially sensitive to large-scale, high-probability motions on longer timescales up to the millisecond regime. The presence of large-scale motions involving the concerted movement of a large number of residues (e.g. inter-domain motion) on such longer timescales can be ascertained qualitatively, since the alignment tensors for the separate domains will be different.[25–27] Ensemble refinement of such systems would have to explicitly include multiple alignment tensors and thus would become more involved. There is also the possibility that there are insufficient data to simultaneously determine both alignment tensors and motion in the absence of additional information.

Acknowledgements

References

1. Kay, L. E. (1998). Protein dynamics from NMR. *Nature Struct. Biol.* **5**, S513–S517.

2. Fisher, M. W. F., Majumdar, A. & Zuiderweg, E. R. P. (1998). Protein NMR relaxation: theory, applications and outlook. *Prog. Nucl. Magn. Reson. Spectrosc.* **33**, 207–272.

3. Ishima, R. & Torchia, D. A. (2000). Protein dynamics from NMR. *Nature Struct. Biol.* **7**, 740–743.

4. Wand, A. J. (2001). Dynamic activation of protein function: a view emerging from NMR spectroscopy. *Nature Struct. Biol.* **8**, 926–931.

5. Palmer, A. G., III (2001). NMR probes of molecular dynamics: overview and comparison with other techniques. *Annu. Rev. Biophys. Biomol. Struct.* **30**, 129–155.

6. Ringe, D. & Petsko, G. A. (1986). Study of protein dynamics by X-ray diffraction. *Methods Enzymol.* **131**, 389–433.

7. Thüne, T. & Badger, J. (1995). Thermal diffuse X-ray scattering and its contribution to understanding protein dynamics. *Prog. Biophys. Mol. Biol.* **63**, 251–276.

8. Karplus, M. & McCammon, J. A. (2002). Molecular dynamics simulations of biomolecules. *Nature Struct. Biol.* **9**, 646–652.

9. Drenth, J. (1994). *Principles of Protein X-ray Crystallography*, Springer, New York.

10. Lipari, G. & Szabo, A. (1982). Model-free approach to the interpretation of nuclear magnetic resonance relaxation in macromolecules. I. Theory and range of validity. *J. Am. Chem. Soc.* **104**, 4546–4559.

11. Palmer, A. G., Grey, M. J. & Wang, C. (2005). Solution NMR spin relaxation methods for characterizing chemical exchange in high-molecular weight systems. *Methods Enzymol.* **384**, 430–465.

12. Tolman, J. R., Al-Hashimi, J. M., Kay, L. E. & Prestegard, J. H. (2001). Structural and dynamic analysis of residual dipolar coupling data for proteins. *J. Am. Chem. Soc.* **123**, 1416–1424.

13. Tolman, J. R. (2002). A novel approach to the retrieval of structural and dynamic information from residual dipolar coupling using several oriented media in biomolecular NMR. *J. Am. Chem. Soc.* **124**, 12020–12030.

14. Briggman, K. B. & Tolman, J. R. (2003). De novo determination of bond orientations and order parameters from residual dipolar couplings with high accuracy. *J. Am. Chem. Soc.* **125**, 10164–10165.

15. Meiler, J., Promper, J. J., Peti, W., Griesinger, C. & Brüschweiler, R. (2001). Model-free approach to the dynamic interpretation of residual dipolar couplings in globular proteins. *J. Am. Chem. Soc.* **123**, 6098–6107.

16. Peti, W., Meiler, J., Brüschweiler, R. & Griesinger, C. (2002). Model-free analysis of protein backbone motion from residual dipolar couplings. *J. Am. Chem. Soc.* **124**, 5822–6833.

17. Hus, J. C., Peti, W., Griesinger, C. & Brüschweiler, R. (2003). Self-consistency analysis of dipolar couplings in multiple alignments of ubiquitin. *J. Am. Chem. Soc.* **125**, 5596–5597.

18. Meiler, J., Peti, W. & Griesinger, C. (2003). Dipolar couplings in multiple alignments suggest alpha helical motion in ubiquitin. *J. Am. Chem. Soc.* **125**, 8072–8073.

19. Bernado, P. & Blackledge, M. (2004). Anisotropic small amplitude peptide plane dynamics in proteins from residual dipolar couplings. *J. Am. Chem. Soc.* **126**, 4907–4920.

20. Bernado, P. & Blackledge, M. (2004). Local dynamic amplitudes on the protein backbone from dipolar couplings: toward the elucidation of slower motions in biomolecules. *J. Am. Chem. Soc.* **126**, 7760–7761.

21. Bouvignies, G., Bernado, P. & Blackledge, M. (2005). Protein backbone dynamics from N–HN dipolar couplings in partially aligned systems: a comparison of motional models in the presence of structural noise. *J. Magn. Reson.* **173**, 328–338.

22. Clore, G. M. & Schwieters, C. D. (2004). How much backbone motion in ubiquitin is required to account for dipolar coupling data measured in multiple alignment media as assessed by independent cross-validation. *J. Am. Chem. Soc.* **126**, 2923–2938.

23. Clore, G. M. & Schwieters, C. D. (2005). Amplitudes of protein backbone dynamics and correlated motions in a small α/β protein: correspondence of dipolar coupling and heteronuclear relaxation measurements. *Biochemistry*, **43**, 10678–10691.

24. Bax, A., Kontaxis, G. & Tjandra, N. (2001). Dipolar couplings in macromolecular structure determination. *Methods Enzymol.* **339**, 127–174.

25. Braddock, D. T., Cai, M., Baber, J. L., Huang, Y. & Clore, G. M. (2001). Rapid identification of medium- to large-scale interdomain motion in modular proteins using dipolar couplings. *J. Am. Chem. Soc.* **123**, 8634–8635.

26. Braddock, D. T., Louis, J. M., Baber, J. L., Levens, D. & Clore, G. M. (2002). Structure and dynamics of KH domains from FBP bound to single-stranded DNA. *Nature*, **415**, 1051–1056.

27. Fischer, M. W., Losonczi, J. A., Weaver, J. L. & Prestegard, J. H. (1999). Domain orientation and dynamics in multidomain proteins from residual dipolar couplings. *Biochemistry*, **38**, 9013–9022.

28. Tolman, J. R., Flanagan, J. M., Kennedy, M. A. & Prestegard, J. H. (1997). NMR evidence for slow collective motions in cyanometmyoglobin. *Nature Struct. Biol.* **4**, 292–297.

29. Pfeiffer, P., Fushman, D. & Cowburn, D. (2001). Simulated and NMR-derived backbone dynamics of a protein with significant flexibility: a comparison of spectral densities for the βARK1 PH domain. *J. Am. Chem. Soc.* **123**, 3021–3036.

30. Henry, E. R. & Szabo, A. (1985). Influence of vibrational motion on solid state line shapes and NMR relaxation. *J. Chem. Phys.* **82**, 4753–4761.

31. Ottiger, M. & Bax, A. (1998). Determination of relative N–H^N, N–C$'$, C$^\alpha$–C$'$ and C$^\alpha$–H$^\alpha$ effective bond lengths in a protein by NMR in a dilute liquid crystalline phase. *J. Am. Chem. Soc.* **120**, 12334–12341.

32. Best, R. B. & Vendruscolo, M. (2004). Determination of protein structures consistent with NMR order parameters. *J. Am. Chem. Soc.* **126**, 8090–8091.

33. Larsen-Lindorff, K., Best, R. B., DePristo, M. A., Dobson, C. M. & Vendruscolo, M. (2005). Simultaneous determination of protein structure and dynamics. *Nature*, **433**, 128–132.

34. Bonvin, A. M. & Brünger, A. T. (1995). Conformational variability of solution nuclear magnetic resonance structures. *J. Mol. Biol.* **250**, 80–93.

35. Bonvin, A. M. & Brünger, A. T. (1996). Do NOE distances contain enough information to access the relative populations of multi-conformer structures. *J. Biomol. NMR*, **7**, 72–76.

36. Gronenborn, A. M., Filpula, D. R., Essig, N. Z., Achari, A., Whitlow, M., Wingfield, P. T. & Clore, G. M. (1991). A novel highly stable fold of the immunoglobulin binding domain of Streptococcal protein G. *Science*, **253**, 657–661.

37. Ulmer, T. S., Ramirez, B. E., Delaglio, F. & Bax, A. (2003). Evaluation of backbone protein positions

and dynamics in a small protein by liquid crystal NMR spectroscopy. *J. Am. Chem. Soc.* **125**, 9179–9191.

38. Derrick, J. P. & Wigley, D. B. (1994). The third IgG-binding domain from streptococcal protein G: an analysis by X-ray crystallography of the structure alone and in a complex with Fab. *J. Mol. Biol.* **243**, 906–918.

39. Hall, J. B. & Fushman, D. (2003). Characterization of the overall and local dynamics of a protein with intermediate rotational anisotropy: differentiating between conformational exchange and anisotropic diffusion in the B3 domain of protein G. *J. Biomol. NMR*, **27**, 261–275.

40. Schwieters, C. D., Kuszewski, J., Tjandra, N. & Clore, G. M. (2003). The Xplor-NIH NMR molecular structure determination package. *J. Magn. Reson.* **160**, 66–74.

41. Kuszewski, J., Gronenborn, A. M. & Clore, G. M. (1999). Inproving the packing and accuracy of NMR structures with a pseudopotential for the radius of gyration. *J. Am. Chem. Soc.* **121**, 2337–2338.

42. Clore, G. M. & Kuszweski, J. (2002). $\chi 1$ rotamer populations and angles of mobile surface side chains are accurately predicted by a torsion angle database potential of mean force. *J. Am. Chem. Soc.* **124**, 2866–2867.

43. Lipsitz, R. S., Sharma, Y., Brooks, B. R. & Tjandra, N. (2002). Hydrogen bonding in high-resolution protein structures: a new method to assess NMR protein geometry. *J. Am. Chem. Soc.* **124**, 10261–10266.

44. Laskowski, R. A., MacArthur, M. W., Moss, D. S. & Thornton, J. M. (1993). PROCHECK: a program to check the stereochemical quality of protein structures. *J. Appl. Crystallog.* **26**, 283–291.

Edited by A. G. Palmer III